

AD-A219 483

DTIC FILE COPY

2

DTIC
ELECTE
MAR 14 1990
D CS D

varian®

QUARTERLY REPORT

for

DARPA/ONR

HIGH TEMPERATURE SUPERCONDUCTIVITY

PERIOD ENDING: December 31, 1989

I. PROGRAM INFORMATION

Contract Number:	N00014-88-C-0760
Principal Investigator:	Dr. James N. Eckstein
Institution/Address	Varian Research Center M.S. K-214 611 Hansen Way Palo Alto, CA 94303 (415) 424-5081
Report Prepared By	Dr. James N. Eckstein
Report Date	March 1, 1990

DISTRIBUTION STATEMENT A
Approved for public release
Distribution Unlimited

90 03 13 175

II. PROGRAM SUMMARY

The overall goals of this program are to develop the technology of MBE growth of HTSC material, to optimize the performance of HTSC films with high-transition temperatures and critical current densities, and to explore the development of electronic devices based on such material.

III. PROGRAM STATUS

The recently developed MBE system is functioning well, and superconducting films with T_c 's above 77K are now routinely being grown, in-situ, by atomic layer epitaxy on both MgO and SrTiO₃. Work is continuing on understanding such issues as required stoichiometric control and methods of improving kinetic control precision, oxidation capacities of reactive oxygen sources, and the effect of crystallographic quality on superconducting properties.

IV ACCOMPLISHMENTS

Most notably, we have continued to improve the superconducting properties of the (BiO)₂-containing layered HTSC films grown in-situ at low temperature without any post-growth anneal. During growth of these films, the crystal surface was monitored by RHEED. When good calibration was achieved so that one burst corresponded to one monolayer, a diffraction pattern characteristic of a single-crystal surface was observed. An example of such a pattern is shown in Fig. 1; the electron beam was incident along the SrTiO₃ (110) direction. The most intense lines are due to a surface periodicity of about 2.7 Å. The fainter lines halfway in between them indicate the a- or b-axis lattice constant of about 5.4 Å. Surrounding the more intense streaks are "side-bands" that are characteristic of an in-plane structure of about 25 Å, presumably due to the non-commensurate b-axis structure modulation. As many as six side-band streaks around each main streak have been observed. In addition, the linewidth of the side-band modulation indicates an in-plane crystallographic coherence

length of more than 150 Å. The patterns evolved in a complex manner reflecting the nature of the instantaneous surface chemistry occurring. In particular, after growth of the bismuth layers in each unit cell, atomically smooth surfaces were observed, as indicated by the RHEED pattern shown here. We have also observed a similar behavior during the growth of 2201, 2212, and 2234 phases.

To further examine the surface morphology, the films were inspected by optical and scanning electron microscopy. Figure 2 shows a SEM picture taken under high magnification and is typical of the kind of structure routinely observed. The film shows a connected, featureless, smooth surface in which small isolated defect structures are observable. The defect size is about 1500 Å or less; their areal density is between 10^6 to 10^8 cm⁻². On films with RHEED patterns that showed evidence for a second phase during growth, a larger density of defects was seen. Other than the isolated defects, the SEM surface images show no evidence of any grain boundary structure. Based on the RHEED patterns observed during and after growth and the plane-view microscopy images, we believe the connected-field region of the film to be single crystal in nature.

After growth, the films were cooled down inside the chamber; a number of cooling regimes were investigated. The highest resistive transition in a 2223 film, directly from the chamber, was 84°K, full zero, and is shown in Fig. 3. This was obtained when the film was cooled from 725°C in the oxygen/ozone flow approximately 20 times that used during growth. The transition seen here is broad, starting above 100°K. Other films have shown onsets above 110°K, but lower values of $T_c(R=0)$. The width of the transition is not understood, and work is underway to sharpen the transition and obtain high transition temperatures. Just above the superconducting transition, the film had a resistivity of about $150\mu\Omega\text{cm}$.

The crystallographic properties of the films were also characterized by X-ray diffraction measurements. Figure 4 shows an X-ray diffraction pattern from a θ -2 θ scan of a superconducting 2223 film; the substrate was tilted 0.5° off of the (001) direction in order to suppress the large

substrate reflections. The film can be indexed to a c-axis lattice constant of 37.2 Å, in good agreement with the range of measured 2223 values. The film is completely epitaxially aligned to the substrate, and there is no evidence of the 2223 phase growth with any other orientation. When the (001) film direction is aligned to the normal scan axis, the widths of the individual film peaks can be used as a measure of the regularity of the atomic layering throughout the film thickness. The linewidths of the (001), (0010) and (0012) peaks indicate coherent Bragg scattering of the incident X-rays from the entire film thickness, which demonstrates the ability of our layered MBE technique to artificially synthesize the crystallographic structure of the film. (The Ag peaks are due to silver paint flakes left over after measuring the film's superconducting transition.)

V PROBLEM AREAS

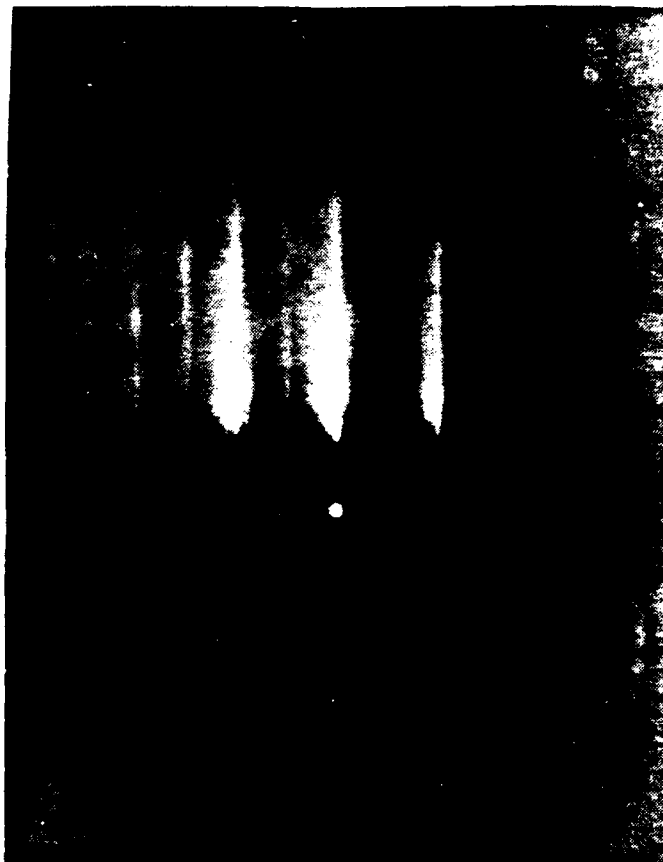
No specific problem areas exist at the present time. More film growth is required to improve film properties and attempt the fabrication of metastable structures.

VI CORRECTIVE ACTION

None required at present

VII GOALS FOR NEXT REPORTING PERIOD

1. To grow atomically-layered, BiO-containing superconducting films with T_c 's above 90K, including metastable structures.



Accession For	
NTIS	CRAQI <input checked="" type="checkbox"/>
DTIC	TAB <input type="checkbox"/>
Unannounced <input type="checkbox"/>	
Justification	
By <i>per AD-A215491</i>	
Distribution	
Availability Codes	
Dist	Avail and/or Special
<i>A-1</i>	



Fig. 1 RHEED pattern along film (100) azimuth during growth of $\text{Bi}_2\text{Sr}_2\text{Ca}_2\text{Cu}_3\text{O}_x$ thin film.

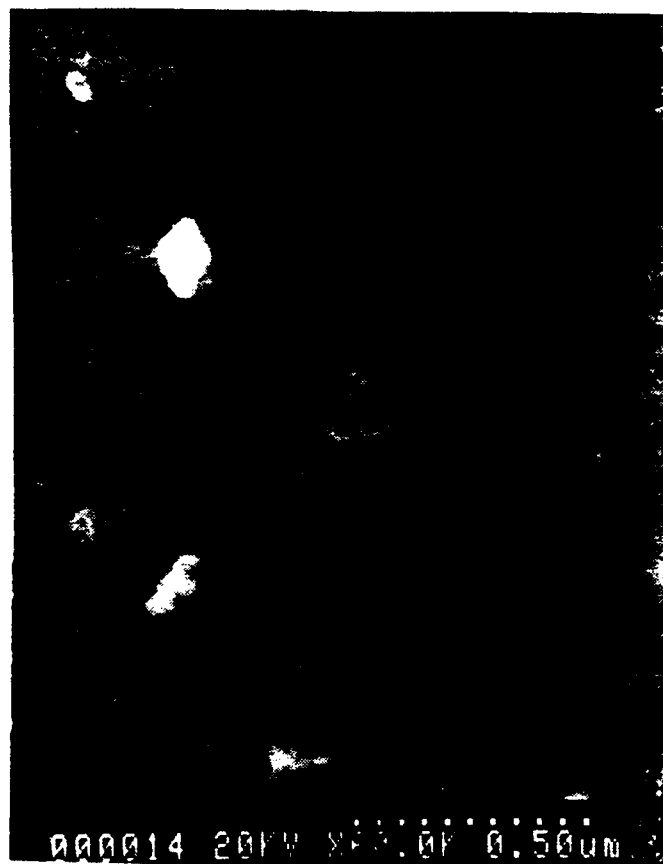


Fig. 2 SEM photograph of surface morphology.

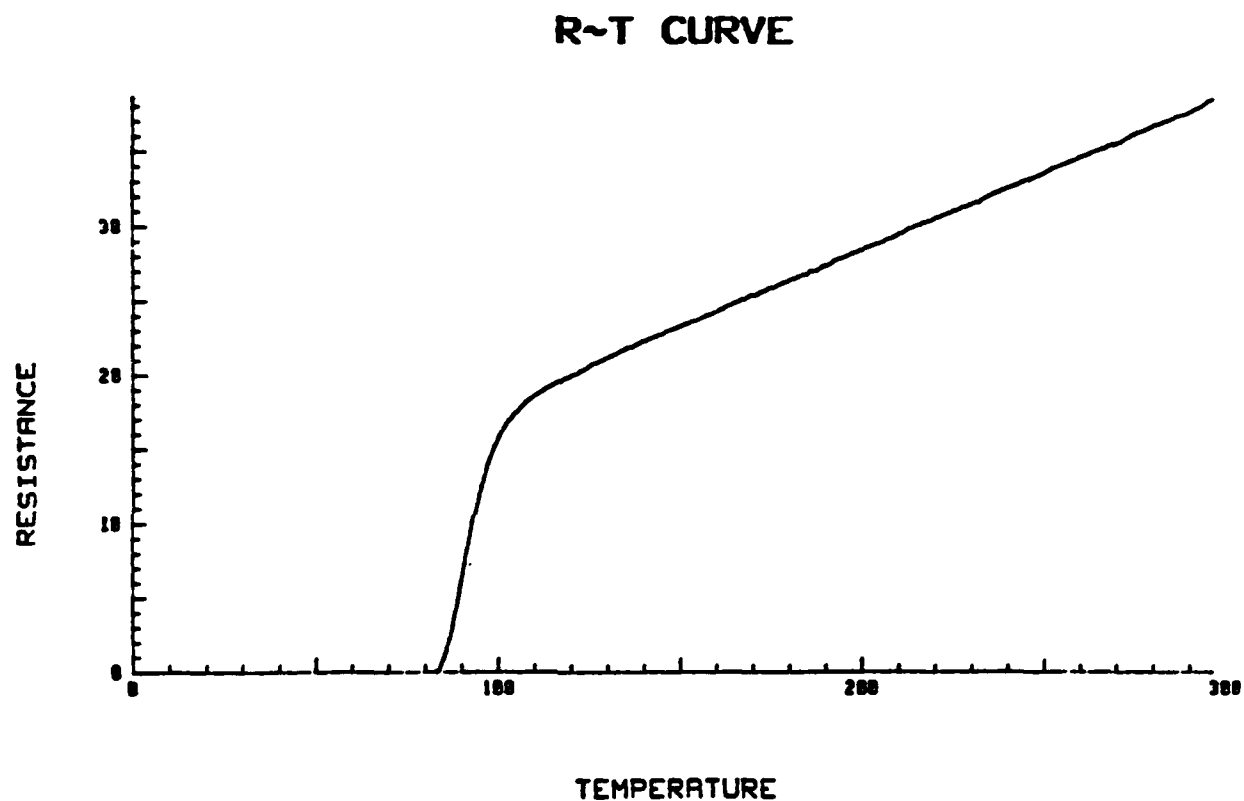


Fig. 3 Superconducting transition at 84K from in-situ-grown $\text{Bi}_2\text{Sr}_2\text{Ca}_2\text{Cu}_3\text{O}_x$ thin film.

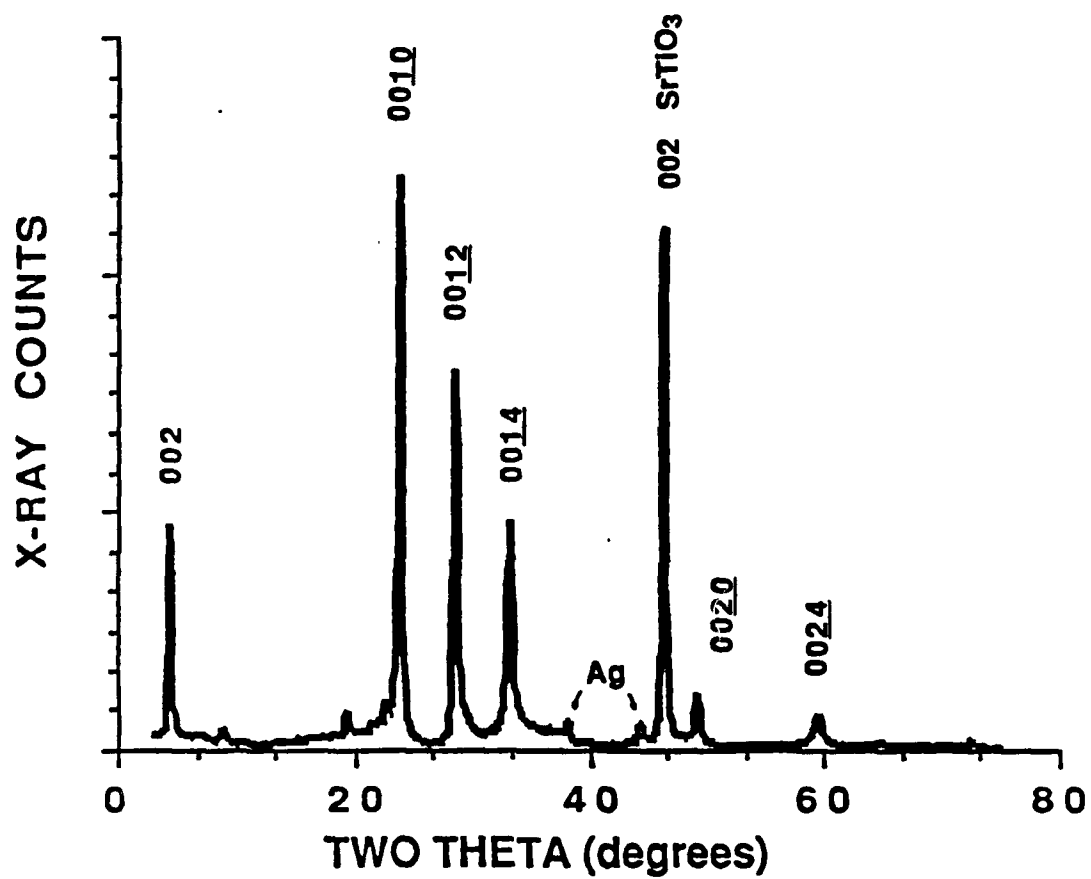


Fig. 4

X-ray diffraction pattern of in-situ-grown $\text{Bi}_2\text{Sr}_2\text{Ca}_2\text{Cu}_3\text{O}_x$ thin film.